K.D. BOUZAKIS, I. MIRISIDIS, N. MICHAILIDIS,
E. LILI, A. SAMPRIS, G. ERKENS, R. CREMER

RESEARCH

PVD Coated Tools' Wear, at Increased Cutting Speeds and Feed Rates, Correlated with Impact Test Results by FEM Simulations

The use of appropriate cutting conditions and coatings is always an issue of pivotal significance since it affects in many ways the overall tool performance in manufacturing processes. To determine optimum conditions, extensive cutting investigations have to be conducted, associated with relatively high expenses. This paper introduces a quick and innovative procedure for characterizing the coating cutting performance, based on the film impact resistance. For the development of this procedure, firstly, it was necessary to conduct milling investigations at various cutting speeds and feed rates. The wear development of tools coated with different films was monitored by SEM investigations and EDX analyses of the cutting edges. In addition, impact tests were conducted at various temperatures and loads and the fatigue strengths of the applied coatings were determined in terms of Woehler diagrams. A quite impressive correlation of the coating impact resistance with the cutting performance at various conditions was established, based on FEM–calculations of the cutting wedge thermal and mechanical loads during the material removal process. Depending on the coated tool and workpiece parameters, there are concrete cutting speed and feed rate regions, which can be effectively detected considering the previously mentioned correlation, leading to an enhanced cutting performance.

Keywords: Coated tools, Impact test, Milling, Wear

1. INTRODUCTION

High mechanical and thermal loadings, especially at increased cutting conditions, i.e. cutting speed and feed rate, are applied on coated tools [1-5]. The investigation of the acting wear phenomena under such cutting conditions is of crucial importance towards obtaining an understanding of the coating failure mechanisms. A cutting performance increase can be achieved through the optimum adoption of cutting conditions to the technical data of the applied tool and coating materials. To determine the optimum conditions, extensive cutting investigations have to be conducted.

Konstantinos-Dionysios BOUZAKIS[1], Ioannis MIRISIDIS[1], Nikolaos MICHAILIDIS[1], Eleftheria LILI[1], Anastasios SAMPRIS[1], Georg ERKENS[2], Rainer CREMER[2]
[1]Laboratory for Machine Tools and Manufacturing Engineering, Mechanical Engineering Department, Aristoteles University of Thessaloniki, 54124 Thessaloniki, Greece
[2]CemeCon AG Adenauerstraße 20 A4 D-52146 Würselen, Germany

The present paper investigates the feasibility of correlating the cutting performance of coated tools with their failure during the impact test at various temperatures [6,7,8]. To that effect, first the coatings' strength properties modifications versus the temperature were detected through appropriate impact test investigations [2,9]. Scanning electron microscope (SEM) observations and energy dispersive X-ray (EDX) analyses facilitated the monitoring of the coating failure start and its development. Furthermore, the wear behavior of coated tools was thoroughly investigated in milling, at increased cutting speeds and feed rates, while taking into account the developed thermal and mechanical loads during the material removal process. The distributions of these loads, in the cutting wedge region, were determined by FEM-calculations, supported by developed FEM-algorithms based on the DEFORM and ANSYS software packages [10,11].

The aim of these investigations was to establish a correlation between the cutting and impact performance of coated tools at various cutting conditions and impact test temperatures, respectively. This correlation can be used to

characterize the cutting performance of PVD-films and moreover, to accelerate the selection of appropriate cutting conditions.

2. APPLIED EXPERIMENTAL PROCEDURES AND DEVICES

2.1 Impact tester

Recent improvements of the impact test rendered feasible the conduct of investigations at elevated temperatures [2,9]. During the impact test a ball penetrates periodically into the coating under a desired maximum load [6,7,8]. The used impact tester, a development of the Laboratory for Machine Tools and Manufacturing Engineering (EEDM) in conjunction with CemeCon AG, allows the application of impact forces up to 1500 N at a frequency of 50 Hz, as well as the ability to determine coatings' Smith and Woehler diagrams, utilizing the ITEC software package [8,12].

2.2 Nanoindentation

Nanoindentation is a precise procedure, during which the course of the gradually applied force versus the displacement is continuously registered. In recent publications [13,14], the "SSCUBONI" (Stress Strain CUrves Based On NanoIndentation) algorithm for the continuous simulation of the nanoindentation was introduced, thus enabling the extraction of materials stress–strain elastic–plastic laws. The nanoindentation device used in the described investigations is a FISCHERSCOPE H100 [15].

2.3 Scanning electron microscopy and milling investigations

A Joel JSM-840 scanning electron microscope, with energy dispersive X-ray analysis facilities, was applied to observe the film failure and extend, as well as the wear development of the coated cutting edges. Further, the cutting investigations were conducted in a numerically controlled 3D milling centre (Johnford, FANUC OM control), by programming circular paths around cylindrical workpieces.

3. APPLIED COATINGS AND DETERMINATION OF THEIR PROPERTIES

Based on the initial development of (Ti,Al)N/(Al,Ti)N nanocomposites with very high aluminium contents [16], the content of aluminium in the Supernitride coating was subsequently reduced to values between 55% for the TINALOX SN^2 coating and 65% for the HYPERLOX coating [17]. The reduction of the Al-content increased the electrical conductivity and thus enabled the use of DC technology for the coating deposition. An additional advantage of the new SN^2 PVD-film is a significantly reduced stress at constant hardness, thus allowing the deposition of thick coatings with increased adhesion. Typical stress values for the SN^2 coating are between -1.2 and -1.7 GPa, compared to about -3 to -4 GPa for conventional TiAlN coatings. A four cathode magnetron sputtering system with additional ionization by plasma booster technology was used.

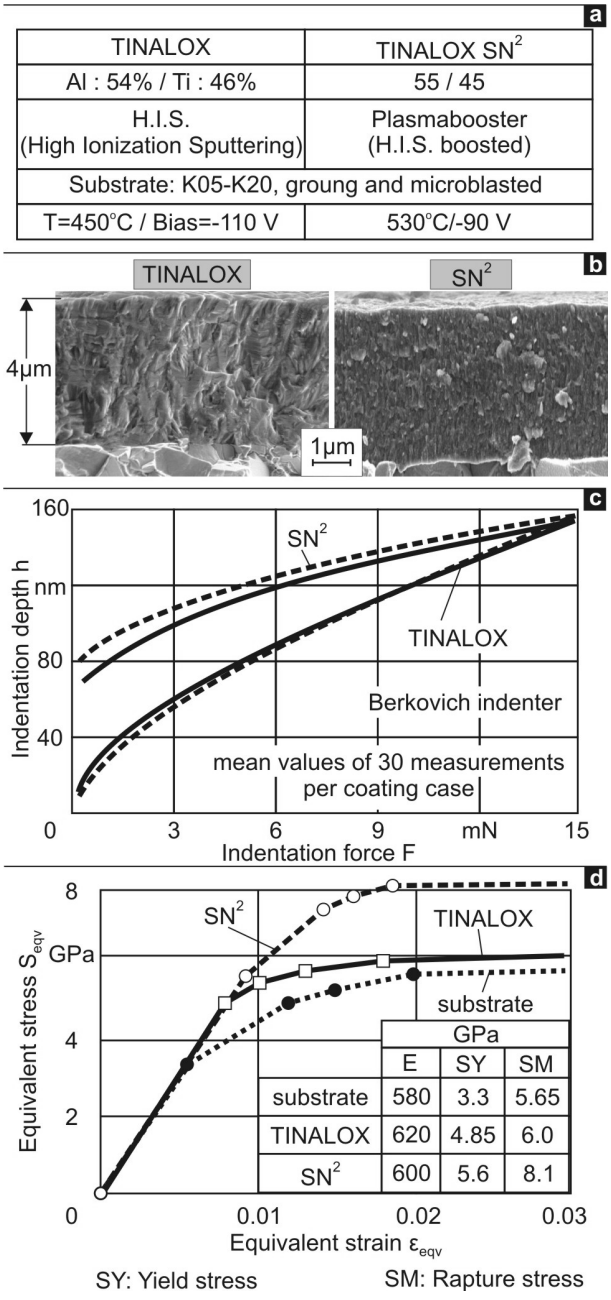

Figure 1: *a: Main specification of the examined coatings and substrate, b: microstructures, c: nanoindentation loading-unloading curves and d: stress-strain curves of the applied films and substrate.*

For film deposition, titanium targets with aluminium plugs were sputtered in an Argon/Nitrogen mixture at a total cathode power of 36 kW and a deposition temperature of 530 °C. Nitrogen flow was controlled by partial pressure measurement and was adjusted to lead to a <111>-texture of the film.

For the investigation's needs, conventional TINALOX and nanocomposite SN^2 films were deposited on K05-K20 cemented carbide inserts. The table in Figure 1a describes the main specifications of the applied coatings, as well as of the substrate. The TINALOX film is based on the High Ionization Sputtering (H.I.S.) technique with an Al/Ti content of 54/46%, while the SN^2 coating is based on an enhanced plasmaboosted H.I.S. deposition procedure with almost the same Al/Ti ratio (53/47%). Figure 1b illustrates the structure of the examined coatings in corresponding cross sections, allowing the visualization of the fine nano-structure of SN^2 film. The mechanical properties of the applied coating and substrate materials were detected by means of nanoindentations and FEM-based algorithms, facilitating the calculation of related stress-strain curves [13,14]. Figure 1c depicts the nanoindentation loading-unloading curves of the coatings which on first sight look almost identical. However, the determined stress-strain curves of the coatings have significant differences mainly in the plastic area (see Figure 1d), with the SN^2 film displaying a superior mechanical strength. The stress-strain curve of the substrate is also included in the same figure.

4. IMPACT PERFORMANCE OF THE INVESTIGATED COATINGS AT ROOM AND ELEVATED TEMPERATURES

The wear propagation of SN^2 coating during the impact test was investigated at operational temperatures up to 400°C and it is monitored in terms of the coating fracture ratio (FR) versus the applied impact force F in Figure 2. Each plotted point corresponds to a test duration of 10^6 impacts. The profile of the coating FR, under various operational temperatures, captures the coating removal rate versus the impact force. The worst performance appears at 300°C and the overall best, at a temperature level of 150°C. At that temperature level the coating withstands up to almost 140 daN to be totally removed (FR = 100%) after 10^6 impacts. Related results for the TINALOX coating were presented in [2].

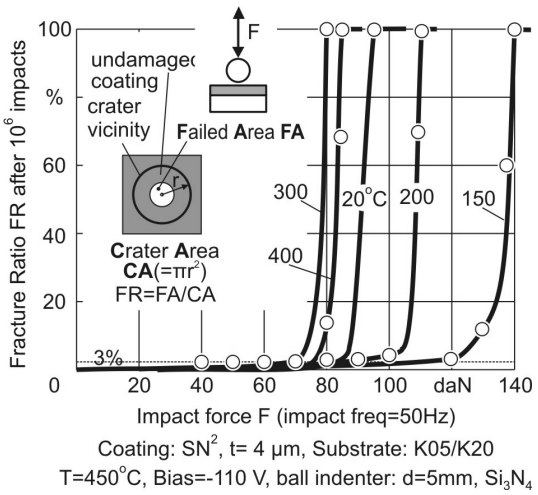

Figure 2: *Coating fracture ratios after 10^6 impacts at various temperatures and loads.*

A plotting of the aforementioned impact behavior of the monitored critical impact force versus the impact temperature up to 600°C is provided in the diagram of figure 3, for the SN^2 coating (solid line) and the TINALOX one (dashed line). Both films demonstrate an enhanced impact resistance at almost 150°C while above this temperature a decreasing tendency of the critical impact load is revealed.

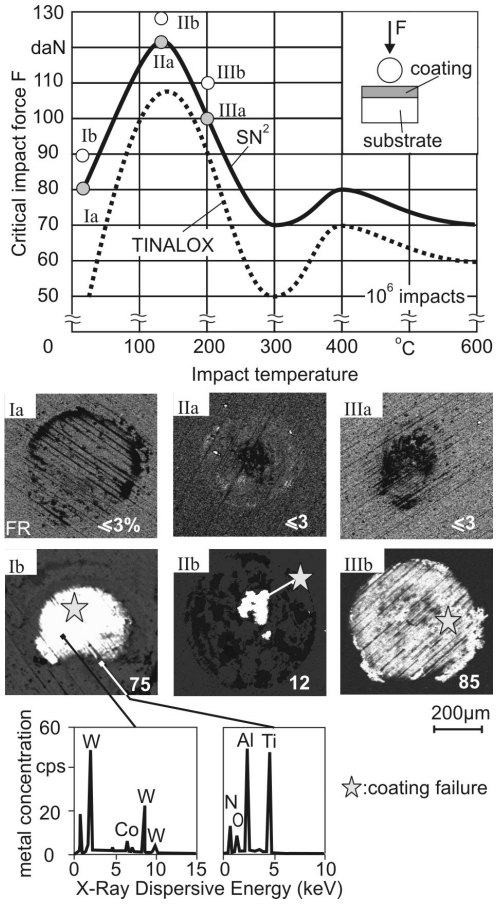

Figure 3: *Critical impact force versus the impact temperature of the examined coatings.*

A second maximum of the impact resistance was encountered at about 400°C; however, this maximum is much lower than the one at 150°C reaching a critical impact force only of 80 and 70 daN for SN^2 and TINALOX coatings, respectively. The film FR increase, after the coating fracture initiation, is less intense at impact temperatures in the region of 100°C to 200°C, compared to all other temperatures, for the same impact force growth of 10 daN, over the corresponding critical load. Thus, the film can withstand repetitive impacts, at temperatures between 100°C and 150°C, for a longer period up to its total removal (FR=100%). The obtained results documented a gradual increase of the coating fatigue strength and thus of the mechanical strength properties for temperatures up to approximately 150°C. This effect may be explained by the dislocations' movements, which are developed within the PVD film under impact loads and the deceleration of their nucleation start [2,18,19], associated with a yield stress increase up to a temperature of ca. 150°C. Over this temperature, it can be assumed that free atoms' diffusion mechanisms antagonistic to the dislocations' movements facilitate the dislocations' nucleation and deteriorate the impact resistance up to approximately 300°C. Moreover, up to ca. 400°C, the film strength properties are improving again, due to the increase of the atoms kinetic energy and hence dislocations' nucleation deceleration. The coating impact resistance is improved near the deposition temperature, due to the release of compressive stresses, induced by the different thermal expansion coefficients of the PVD films and their substrates, at temperatures lower than the deposition temperature. Over 400°C up to 600°C, no phase transformations take place [20]. On the other hand, a hardness reduce [21] and oxidation mechanisms activation [18,19,20,22,23] affect the coating strength properties and impact resistance. Experimental evidences of the aforementioned SN^2 film impact behavior are presented in the SEM micrographs and EDX analysis of the same figure.

5. WEAR BEHAVIOR OF COATED TOOLS IN MILLING AT VARIOUS CUTTING SPEEDS AND FEED RATES

The conduct of cutting experiments was necessary to investigate a potential correlation of the wear performance with the impact resistance of coated tools at various temperatures. The hardened steel 42CrMo4 V was used as the workpiece material in these investigations.

5.1 Wear development at various cutting speeds

Cemented carbide inserts coated with SN^2 films, with the same specifications as the ones used in the previously described impact tests, were applied in milling to monitor the coating wear phenomena at various cutting speeds up to 600 m/min. The cutting strategy is presented in Figure 4a. After certain number of cuts, the flank wear VB was measured and the wear development in the cutting wedge region was documented by SEM photos and EDX-microanalyses. A synopsis of the achieved

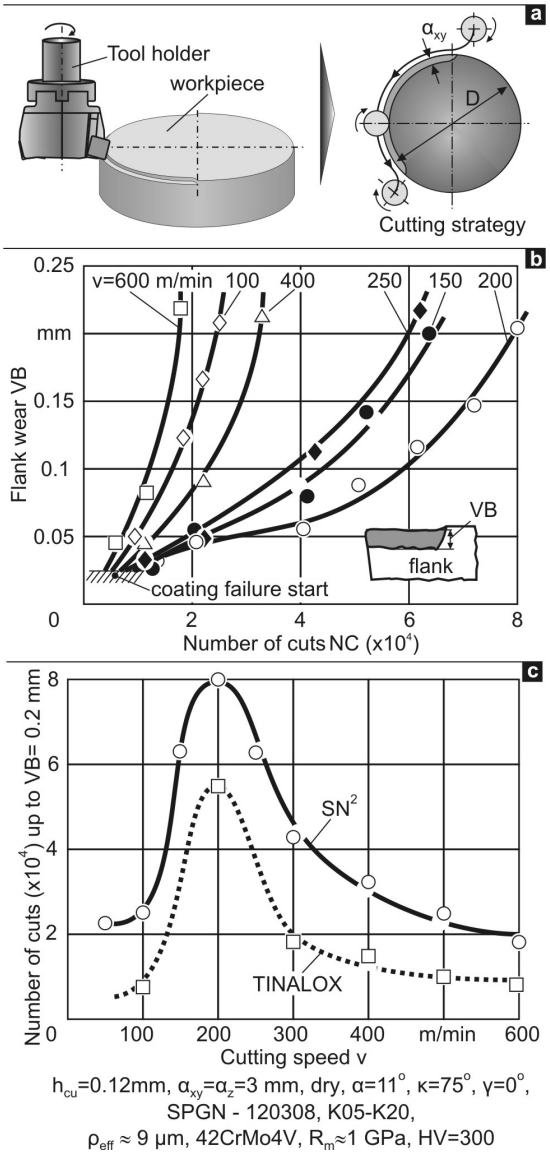

Figure 4: *a: Milling kinematics, b: Flank wear versus the number of cuts and c: number of achieved cuts up to VB= 0.2 mm, at various cutting speeds.*

results is displayed in Figure 4b, where the development of the flank wear VB versus the number of cuts is exhibited for various cutting

speeds. The overall best cutting performance is achieved at the cutting speed of 200 m/min, attaining a flank wear of 0.2 mm, after approximately 80.000 cuts. It is worthwhile pointing out that a steep wear increase versus the number of cuts was achieved at the lowest cutting speed of 100 m/min, comparable to that one at the cutting speed of 600 m/min. The number of cuts obtained up to a flank wear VB of 0.2 mm at various cutting speeds is captured in Figure 4c. There is a significant increase of the cutting tool performance at the cutting speed of 200 m/min. This effect can be attributed to the improvement of the film impact resistance and strength properties at a cutting temperature between 100°C and 200°C; this insight is further supported by calculations, which are described in the following section. A common cutting behavior was also encountered in the TINALOX coating case, as described in [2] and plotted in the same diagram with a dashed line.

5.2 Wear development at various feed rates

The flank wear development in milling, at a low and an increased feed rate corresponding to undeformed chip thickness h_{cu} of 0.12 mm and 0.4 mm respectively, is displayed in Figure 5.

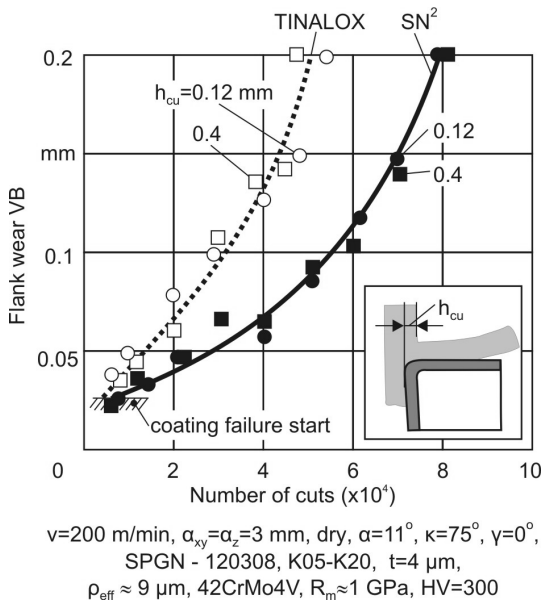

Figure 5: *Flank wear development versus the number of cuts, for various undeformed chip thicknesses in milling.*

The feed rate growth practically did not affect the tool flank wear versus the number of cuts. In both feed rate cases a flank wear of 0.2 mm was attained after approximately $5.5x10^4$ cuts for the TINALOX coating [3] and $8x10^4$ cuts for the SN^2 film. On the other hand, the flank wear develops significantly slower versus the removed material volume when increasing the feed rate [3]. This occurs since in the case of an undeformed chip thickness h_{cu} of 0.4 mm in both coating cases, a practically four times higher removed material volume per cutting length was obtained, up to the same flank wear of 0.2 mm, in comparison to a h_{cu} of 0.12 mm. In this way, through the feed rate increase an impressively higher cutting performance can be achieved, without reducing the tool life; this behavior will be further discussed in the next section.

5.3 Explanation of the coated tools' wear phenomena at various cutting speeds and feedrates

Considering SEM micrographs of the coated cutting wedge, at early flank wear stages of ca. 0.05 mm, as well as, wear results of previous investigations [22], the coating wear development at various cutting speeds can be described schematically by the upper part of Figure 6.

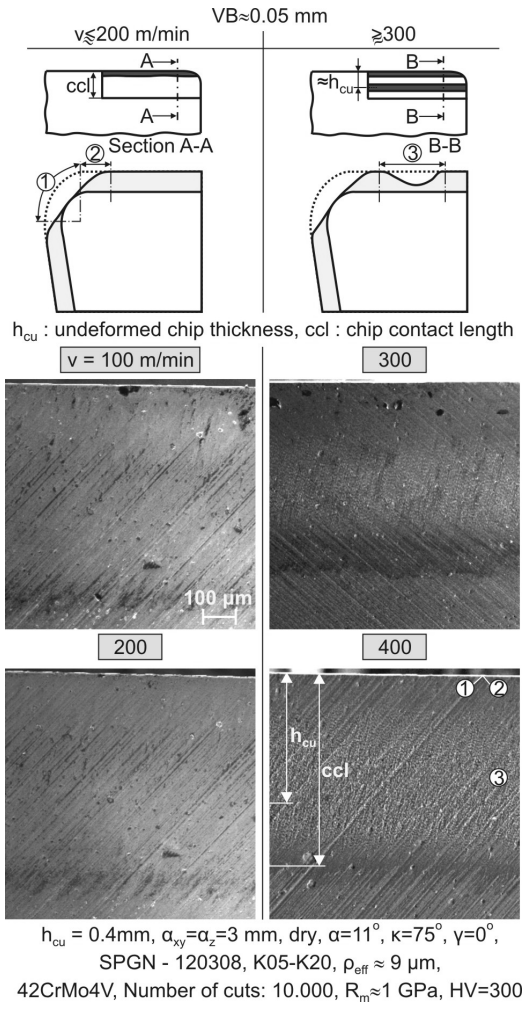

Figure 6: *Coating failure phenomena at a low flank wear, verified by SEM micrographs, at various cutting speeds.*

In all the examined cases, coating failures start on the curvature of the cutting wedge (locations 1 and 2). At higher cutting speeds (>≈ 300 m/min), an additional coating damage is developed on the rake (location 3).

This coating failure is simultaneous to the described ones, appearing on the curvature of the cutting wedge and can be dominant for the tool life at cutting speeds higher than ca. 300 m/min.

The SEM micrographs at the bottom of the figure, presenting the wear status of the tool rake, coated with a SN^2 film, after 10.000 cuts up to a cutting speed of 400 m/min, verify the introduced wear propagation phenomena. Similar results were obtained in the case of TINALOX coating, as presented in [2,3].

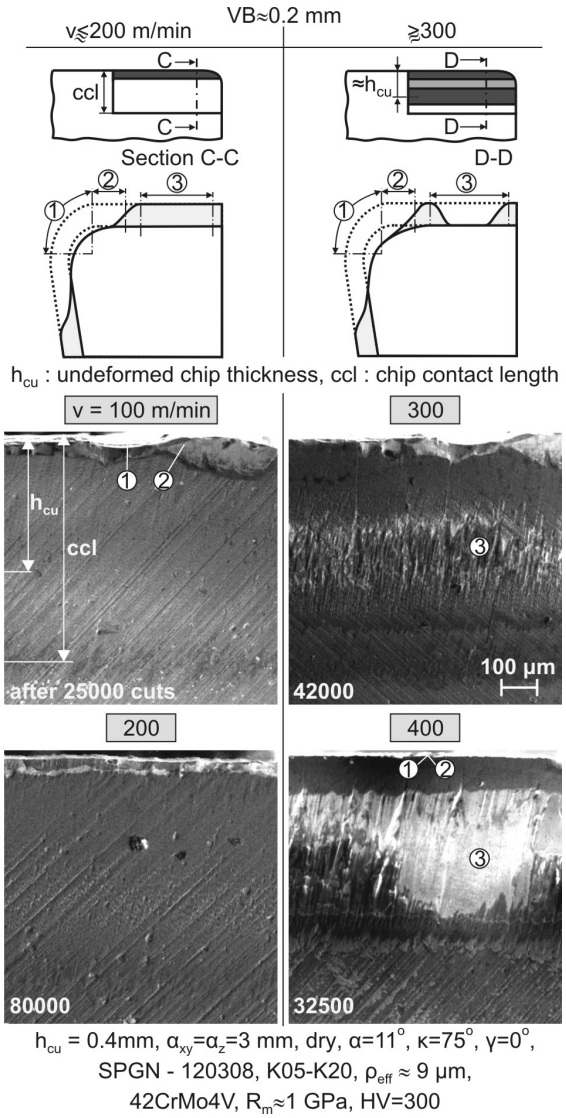

Figure 7: *Coating failure phenomena at a flank wear of 0.2 mm, verified by SEM micrographs, at various cutting speeds.*

At higher flank wear stages up to 0.2 mm, the coating removal on the cutting wedge is complete; however, this occurs at significantly higher number of cuts, at cutting speeds of 200 m/min. The upper part of Figure 7 illustrates schematically the increased coating failure, which at low cutting speeds, i.e. lower than 200 m/min, is limited to the cutting wedge but at higher than 300 m/min the coating failure is extended to a major part of the chip contact on the tool rake.

The SEM micrographs shown in the bottom figure part, further verify this coating wear mechanisms. It is obvious that a coating failure takes place both on the flank and the rake at the indicated wedge locations 1 and 2, but the wear extent and the number of the achieved cuts up to VB ≈ 0.2 mm varies, depending on the cutting speed, due to the different mechanical and thermal loads, which will be tackled theoretically in the next section, by FEM simulation of the cutting process. Based on these FEM calculations, a correlation between the described wear mechanisms of the coated inserts in milling and in impact test will be established.

6. CORRELATION OF THE WEAR DEVELOPMENT AT VARIOUS CUTTING SPEEDS AND FEED RATES TO THE IMPACT RESISTANCE, BASED ON FEM CALCULATIONS

In order to obtain insights of the developed temperature field and of the acting mechanical loads distributions in the cutting wedge region, during the material removal, FEM calculations of the cutting process were conducted at various cutting speeds and feed rates by algorithms developed by the research team, based on the DEFORM and ANSYS software packages [10,11]. Figure 8a demonstrates the applied FEM model to determine the temperature field in the cutting wedge region, where input data are the undeformed chip thickness h_{cu}, the cutting speed, as well as the coating, the substrate and the workpiece material properties. The applied friction in DEFORM software package is described by the shear friction coefficient. This coefficient was appropriately selected to the value of 0.6, by trial and error method, so as to have a convergence of the calculated force components with the measured ones in milling [2,3]. A chip-cutting wedge cross-section and an indicative temperature field distribution are displayed within the chip contact length (ccl). The illustrated temperature distribution appears after the cutting of a chip length corresponding to the length of the formed

chips in the conducted milling investigations. For simplicity reasons, the chip thickness remains stable throughout the chip length. Figure 8b displays the temperature in three distinct regions of the coating versus the cutting time. In positions 1 and 2, which correspond to the bottom and the upper limit of the rounded cutting wedge region respectively, the coating temperature is almost the same, as shown versus the cutting time (~cutting length) in the left diagram of Figure 8b.

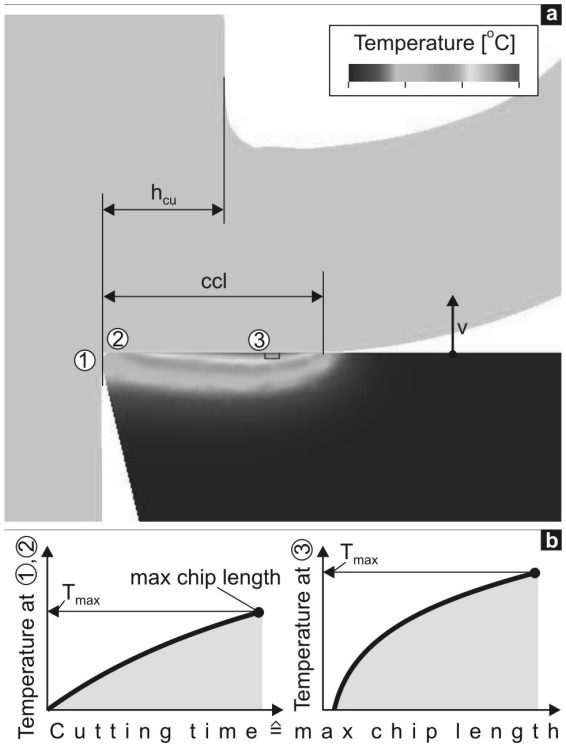

Figure 8: *a: FEM simulation of the chip shape and temperatures distributions within the coated tool considering the cutting speed and the feed rate (DEFORM-based calculations). b: The temperature development on the coating over the cutting time (~cutting length).*

The temperature in position 3, which corresponds approximately to the position where the undeformed chip thickness h_{cu} ends, follows a course versus the cutting time, as illustrated in the diagram in the right hand side of the figure.

The maximum calculated temperature varies, depending on the cutting speed and feed rate as well as on the location on the tool rake, as illustrated in Figure 9.

The developed maximum temperatures in positions 1 and 2 amount to approximately 60°C at a cutting speed of 100 m/min and a h_{cu} of 0.12 mm (see upper diagram of the figure), and then exhibits an almost stable course versus the cutting speed, reaching a temperature of ca. 200°C. On the other hand, at the indicated location 3, the film thermal load is maximized and the temperature has an increasing tendency versus the cutting speed, attaining the value of 590°C, at the cutting speed of 600 m/min. The corresponding results obtained for the developed maximum temperatures versus the cutting speed at a h_{cu} of 0.4 mm, are presented in the bottom diagram of the figure.

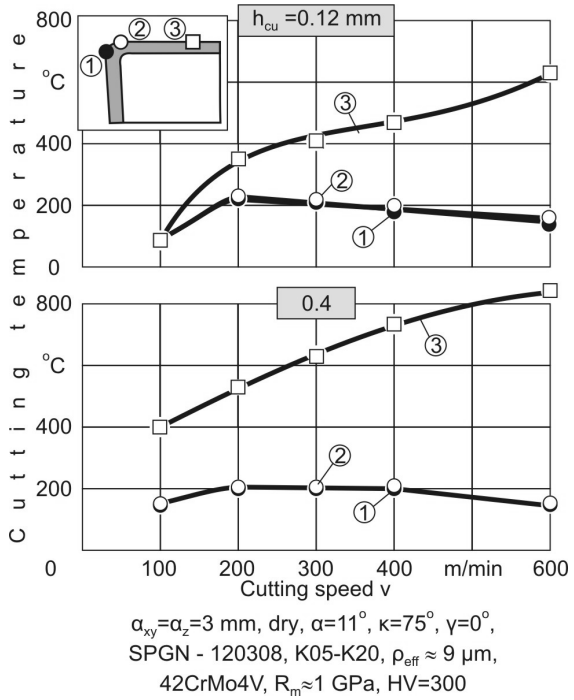

Figure 9: *Temperature distributions within the coated tool considering the cutting speed and the feed rate at three distinct positions of the cutting wedge.*

The examined coatings' mechanical properties modifications, in terms of Woehler diagrams and stress-strain curves, due the increase of the temperature, were determined by the procedures explained in [2,3], employing the ITEC software [8]. Figure 10a demonstrates the impact fatigue strength increase of both coatings at a temperature of 200°C, compared to room temperature. Accordingly, Figure 10b presents the increasing of coatings' yield strength at the same temperature, with the Young's moduli of both coatings remaining stable over the temperature increase up to 200°C.

The applied coating and substrate elasticity moduli in the relevant calculations were determined after the methodology described in [14] at room temperatures, based on nanoindentations. Furthermore, it was assumed that the film yield and rapture stresses at 200°C were increased with regard to the room temperature, as the endurance stress growth from room temperature up to 200°C.

The presented Woehler diagrams were applied to obtain an insight of the film fracture initiation in milling with coated tools, at various cutting speeds and feed rates.

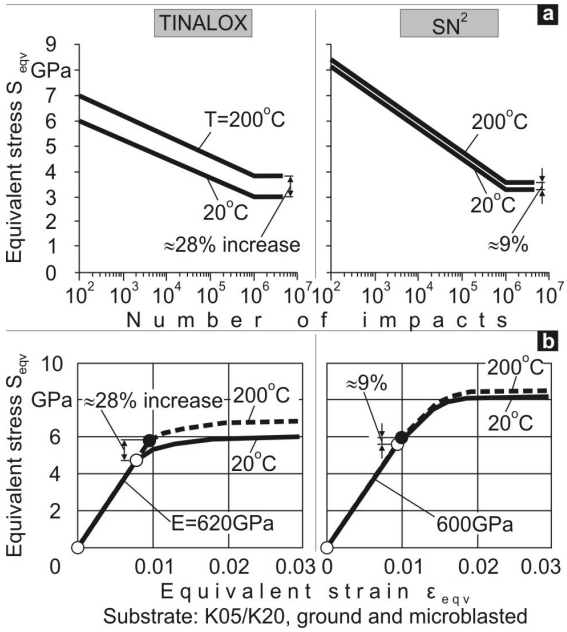

Figure 10: *a: Woehler diagrams of the examined coatings and b: corresponding stress-strain curves at room and elevated temperatures*

Taking into account the measured cutting forces and chip contact lengths, the stresses developed in the cutting wedge can be determined, employing the FEM simulation model of the material removal process, supported by the ANSYS software [11], as explained in [24]. To increase the calculations' accuracy the cutting force distributions on the rake were determined through DEFORM-based calculations and the resulting cutting pressure distributions were considered in ANSYS FEM-models. These distributions were multi-linearly approximated and were adapted to the measured ccl, $F_{\kappa n}$ and F_c values [24]. The FEM modeling strategy of the coated cutting wedge and of its loads during the material removal process is illustrated in Figure 11a. The coated cutting wedge is generally described by a plain strain model [2]. The acting cutting loads are applied in a form of superficial normal and tangential pressure distributions, determined taking into account the measured cutting forces and the chip contact length. The stress distributions in the cutting wedge region are demonstrated in Figure 11b for an undeformed chip thickness of 0.12 mm for both the examined coatings. Furthermore, the corresponding results for a h_{cu} of 0.4 mm are provided in Figure 11c. According to these results, the feed rate increase does not affect practically the developed maximum stresses, appearing in both feed rate cases on the cutting wedge transient region close to the flank. The stresses are slightly higher in the case of TINALOX coating, due to its higher Young's modulus. By inserting the developed stresses in the corresponding coating's Woehler diagrams, a prediction of the first coating failure in the transient region of the cutting wedge close to the flank, where the maximum stresses occur, can be attained (see Figure 11d).

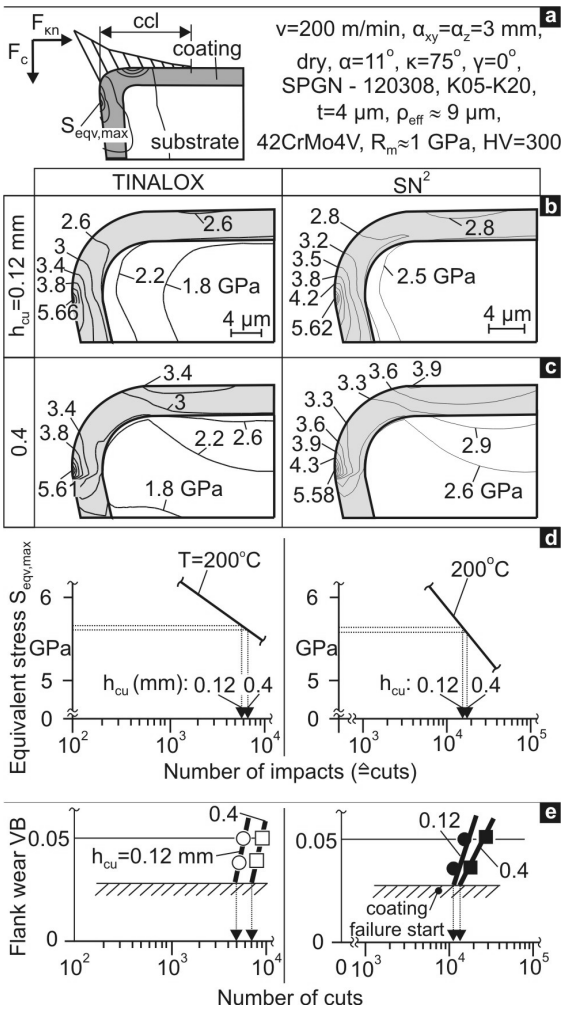

Figure 11: *a: The applied cutting loads on the cutting wedge, in terms of force distributions. b: Stress distributions on the cutting wedge for undeformed chip thicknesses of 0.12 mm and c: of 0.4 mm. d: Coating failure initiation prediction, employing the determined stresses on the cutting wedge and the coating Woehler diagrams at various temperatures. e: Experimentally determined first coating failure.*

The expected coating failure startup for the case of an undeformed chip thickness of 0.12 mm are approximately $6x10^3$ and $1.1x10^4$ cuts for TINALOX and SN^2 films, respectively. On the other hand, the corresponding prediction for film

failure initiation at a h_{cu} of 0.4 mm leads to $7x10^3$ and $1.1x10^4$ cuts for the same coating cases. These expectations are in good agreement with the experimental results presented in Figure 11e (see also figure 4b), where the captured through SEM observations flank wear when the first coating failure appears, is depicted versus the number of cuts.

The possibility to calculate the developed temperature during material removal, allows the correlation between the coating impact resistance with the tool wear results obtained in milling, at various cutting speeds and feed rates for both the examined coating cases. Such relationships are demonstrated in Figures 12a and 12b, for feed rates corresponding to undeformed chip thickness values of 0.12 and 0.4 mm respectively. The critical force after 10^6 impacts at a coating fracture ratio less than 3% and the number of the achieved cuts up to a flank wear of 0.2 mm are exhibited, versus the cutting speed and the impact test temperature.

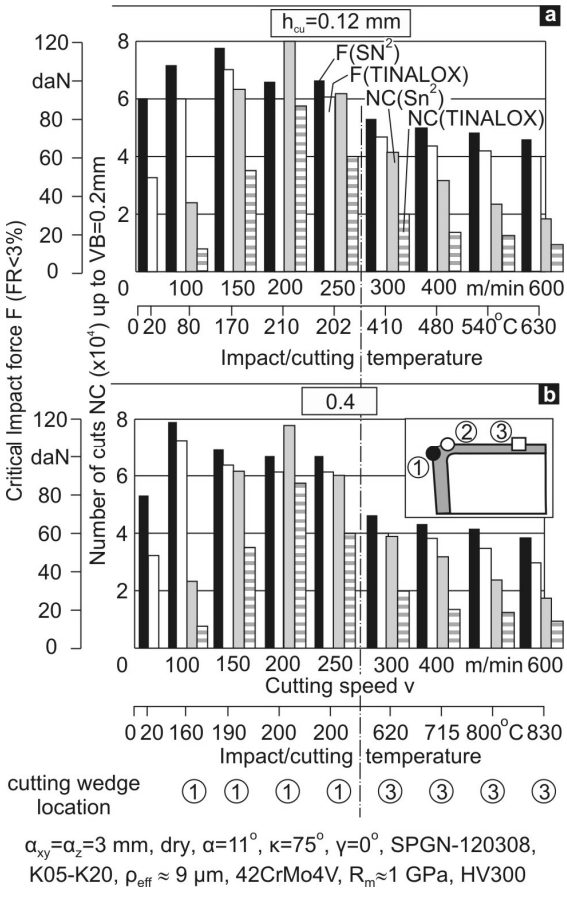

Figure 12: *a: Correlation between cutting performance and coating impact resistance for TINALOX and SN² films, at a feed rate of 0.12 mm and b: 0.4 mm.*

The recorded impact test temperatures according to the conducted FEM calculations correspond to the cutting speeds and tool wedge location, as displayed in the figure. In the investigated coated cutting tool - workpiece material cases, up to a cutting speed of approximately 300 m/min, the cutting wedge wear at the transient region from the flank to the rake, determines the tool performance. Over 300 m/min, the wear on the rake location 3 is dominant for the achieved number of cuts. It is quite impressive that there is an almost identical behavior of the coating cutting performance versus the cutting speed with the impact test resistance versus the temperature in both film and feed rate cases. The possibility to calculate cutting temperatures on the tool surface and to correspond them to coatings mechanical properties, taking into account impact test results, as shown in figure 12, allows the prediction of the cutting speed regions associated with improved wear behaviors.

7. CONCLUSIONS

The effect of the cutting speed and the feed rate on the milling performance of tools coated with various PVD-films was investigated in the current paper. The results revealed that at a concrete cutting speed the coating performance is maximized at low and high feedrates. This behavior can be attributed to the developed stress fields in the cutting wedge region in combination with the modification of the coating mechanical properties, due to the encountered cutting temperatures. The film mechanical properties modifications were detected by impact tests versus the temperature. FEM calculations of the material removal process explained the experimental results in milling, thus allowing a satisfactory correlation of the coating cutting performance at various cutting speeds and feedrates with the temperature dependent film impact resistance.

8. ACKNOWLEDGEMENTS

The authors would like to thank Kennametal GmbH for providing the cemented carbide inserts used in the described investigations.

9. REFERENCES

[1] F. Klocke, T. Krieg, *CIRP Annals – Manufacturing Technology*, 1999, 42/2, 515.

[2] K.-D. Bouzakis, I. Mirisidis, E. Lili, N. Michailidis, A. Sampris, G. Skordaris, E. Pavlidou, G. Erkens, I. Wirth, *CIRP Annals – Manufacturing Technology*, 2006, 55/1, 67.

[3] K.-D. Bouzakis, I. Mirisidis, N. Michailidis, E. Lili, A. Sampris, G, Erkens, R. Cremer, *Plasma Processes & Polymers*, 2007, 4, 301.

[4] H. K. Toenshoff, A. Mohlfeld, *Int. J. Mach. Tools Manufact.*, 1998, 38, 469.

[5] *"Handbook of Hard Coatings"*, R. Bunshah, Noyes Publicationsy William Andrew Publishing, New York 2001.

[6] O. Knotek, B. Bosserhoff, A. Schrey, T. Leyendecker, O. Lemmer, S. Esser, *Surface and Coatings Technology*, 1992, 54–55, 102.

[7] J.C.A. Batista, C. Godoy, A. Matthews, *Surface and Coatings Technology*, 2003, 163–164, 353.

[8] K.-D. Bouzakis, N. Michailidis, A. Lontos, A. Siganos, S. Hadjiyiannis, G. Giannopoulos, G. Maliaris, T. Leyentecker, G. Erkens, *Zeitschrift fuer Metallkunde*, 2001, 92, 1180.

[9] K.-D. Bouzakis, E. Lili, A. Sampris, N. Michailidis, E. Pavlidou, G. Skordaris, Impact test on PVD coatings, at elevated temperatures, Proceedings of 5th International Conference "THE Coatings" 5-7 October 2005 Kallithea, Halkidiki, Greece, ISBN 960-243-616-6, 311-322, 2005.

[10] Operational manual, DEFORM 2005.

[11] SWANSON Analysis System, INC., ANSYS user manuals, Vol.1 Theory, Vol.2 Procedures, Vol.3 Elements, Vol.4 Commands, 2006.

[12] EEDM/CemeCon AG, Impact tester manual, 2006.

[13] K.-D. Bouzakis, N. Michailidis, S. Hadjiyiannis, G. Skordaris, G. Erkens, *Materials Characterization*, 2003, 49, 149.

[14] K.-D. Bouzakis, N. Michailidis, G. Erkens, *Surface and Coatings Technology*, 2001, 142-144, 102.

[15] HELMUT FISCHER GmbH+Co Evaluation Manual of Indentation, Procedure, Sindelfingen-Germany, (2000).

[16] G. Erkens, R. Cremer, T. Hamoudi, K. -D. Bouzakis, I. Mirisidis, S. Hadjiyiannis, G. Skordaris, A. Asimakopoulos, S. Kombogiannis, J. Anastopoulos and K. Efstathiou, *Surface and Coatings Technology*, 2004, 177-178, 727.

[17] CemeCon facts No. 24, September 2005.

[18] A. Hörling, L. Hultman, M. Odén, J. Sjölén, L. Karlsson, Surface and Coatings Technology, 2005, 191, 384.

[19] E. Schäffer, G. Kleer, *Surface and Coatings Technology*, 2000, 133-134, 215.

[20] K.-D. Bouzakis, G. Skordaris, I. Mirisidis, N. Michailidis, G. Mesomeris, E. Pavlidou, G. Erkens, *Surface and Coatings Technology*, 2005, 200, 1879.

[21] D.T. Quinto, G.J. Wolfe, P.C. Jindal, *Thin Solid Films*, 1987, 153, 19.

[22] K.-D. Bouzakis, N. Vidakis, N. Michailidis, T. Leyendecker, G. Erkens, H.-G. Fuss, *Surface and Coating Technologies*, 1999, 120/121, 34.

[23] R. Cremer, M. Witthaut, A. von Richthofen, D. Neuschutz, *Thin Films Coat. Ecasia*, 1997, 97, 963.

[24] J. Anastopoulos, Cutting tools' life improvement through PVD coatings with mono and multilayer structures, with different chemical compositions, as well as mechanical properties, Aristoteles University of Thessaloniki, PhD thesis, ISBN 960-243-624-7, 2006.